PCCP

Cite this: *Phys. Chem. Chem. Phys.*, 2011, **13**, 12225–12230

www.rsc.org/pccp

PAPER

Adsorption of DNA/RNA nucleobases on hexagonal boron nitride sheet: an *ab initio* study

Qing Lin, Xiaolong Zou, Gang Zhou, Rui Liu, Jian Wu, Jia Li* and Wenhui Duan*

Received 16th March 2011, Accepted 26th April 2011
DOI: 10.1039/c1cp20783k

Our *ab initio* calculations indicate that the interaction of deoxyribonucleic/ribonucleic acid (DNA/RNA) nucleobases [guanine (G), adenine (A), thymine (T), cytosine (C), and uracil (U)] with the hexagonal boron nitride (*h*-BN) sheet, a polar but chemically inert surface, is governed by mutual polarization. Unlike the case of graphene, all nucleobases exhibit the same stacking arrangement on the *h*-BN sheet due to polarization effects: the anions (N and O atoms) of nucleobases prefer to stay on top of cations (B) of the substrate as far as possible, regardless of the biological properties of nucleobases. The adsorption energies, ranging from 0.5 eV to 0.69 eV, increase in the order of U, C, T, A and G, which can be attributed to different side groups or atoms of nucleobases. The fundamental nature of DNA/RNA nucleobases and *h*-BN sheet remains unchanged upon adsorption, suggesting that the *h*-BN sheet is a promising template for DNA/RNA-related research, such as self-assembly.

I. Introduction

The self-assembly of deoxyribonucleic acid (DNA) bases on the template has been hypothesized to play a crucial role in the emergence of life under prebiotic conditions.[1–4] Generally, it is of great importance that the templates used should have well-defined surface structure and stable property, and meanwhile should not change the essential properties of the DNA film. So far, most work has been focused on the homogeneous surface such as metal[5,6] and graphite surfaces.[7,8] It was found previously that graphite could be a suitable candidate for the detection of single molecules and intermolecular interactions in virtue of sophisticated surface analysis techniques[9] because of its inert nature. In contrast, information on the heterogeneous surface as the template for the self-assembly or detection of DNA is relatively scarce.

Hexagonal boron nitride (*h*-BN) is viewed as the analogue of graphite because they are isoelectronic and have identical honeycomb structure. However, *h*-BN is a wide band-gap polar semiconductor with high thermal and chemical stability due to the charge transfer between the constituent B and N atoms.[10] Recently, mono- and few-layer *h*-BN sheets were successfully prepared by the micromechanical cleavage method[11] and chemical-solution-derived method[12] without introducing the metal substrate, exhibiting electronic properties similar to those of the *h*-BN surface.[12,13] Free-standing single-layer BN sheet has been fabricated *via* controlling energetic electron beam irradiation through a sputter process.[14,15] These breakthrough experiments may pave the way for future applications of the *h*-BN sheet in many fields, such as electronic devices and templates for assembling specific nanostructures.[16–18] Intuitively, the adsorption of DNA on the monolayer *h*-BN sheet should be a good candidate to study the self-assembly of DNA on the heterogeneous template.

In this paper, within the framework of density-functional theory (DFT), we investigated the adsorption of five common DNA/Ribonucleic acid (RNA) nucleobases, including guanine (G), adenine (A), thymine (T), cytosine (C) and uracil (U), on the monolayer *h*-BN sheet. We obtained the stable configurations of the nuclebases on *h*-BN sheet, which are found to be different from those on metal surface or graphene (homogeneous templates), and the noncovalent interaction nature between nuclebases and *h*-BN sheet. Such noncovalent functionalization of the *h*-BN sheet with the nucleobases, which induces a moderate adhesive force to immobilize nuclebases on the sheet without damaging essential properties of the sheet and nuclebases, would be useful for practical self-assembly of the DNA/RNA. It would also be advantageous for the growth of a perfect DNA-BN hybrid for future device applications under diverse environments, like carbon nanotube (CNT) DNA sensors[19] and graphene-based single-bacterium resolution biodevice and DNA transistor[20] reported recently.

II. Calculation method and model

All calculations in this work were performed using the Vienna *ab initio* Simulation Package (VASP).[21,22] The ultrasoft pseudopotentials[23] for the electron-ion interaction and the

Department of Physics, Tsinghua University, Beijing 100084, People's Republic of China. E-mail: dwh@phys.tsinghua.edu.cn; lijia@phys.tsinghua.edu.cn

local density approximation (LDA)[24] for the exchange–correlation potential were used. Previous works have shown that DFT within LDA can successfully describe the overall adsorption characteristics of some DNA bases on graphene[25] and CNTs.[26] The cut-off energy for the plane-wave basis set was 400 eV. We adopted a hexagonal 5 ×5 × 1 supercell[27] for the *h*-BN sheet, where a vacuum region of 15 Å between adjacent *h*-BN sheets was employed to eliminate the sheet-sheet interactions. The base molecules were terminated at the cut bond to the sugar ring with a methyl group to generate an electronic environment in the nucleobase similar to the situation in DNA/RNA.[25] Integration over the Brillouin zone is done using a single Gamma *k*-point for the atomic structure relaxation and the Monkhorst–Pack scheme with 6 × 6 × 1 *k*-point meshes for electronic structure calculation. The energy and force convergence criteria were 10^{-5} eV and 0.005 eV $Å^{-1}$, respectively.

To explore possible self-assembly process of DNA/RNA on the BN template, it is important to first identify the adsorption behavior of nucleobases on *h*-BN sheet. In terms of the previous work on the adsorption of adenine and thymine on CNTs[26] and considering the unique structural characteristics of *h*-BN sheet, we adopted five initial adsorption configurations with different relative positions between the primary hexagonal ring of the nucleobase and the *h*-BN hexagonal rings in the structural optimization (Fig. 1a). These adsorption configurations are classified as (i) Top^B and Top^N, where the center of the nucleobase primary hexagonal ring is on top of the B atom or N atom of the BN sheet, as shown in Fig. 1b and c respectively; (ii) $bridge^{NB}$ and $bridge^{BN}$, where the center of the nucleobase primary hexagonal ring is at the BN bridge site as shown in Fig. 1d and e respectively; and iii) the hollow (Fig. 1f). In all cases, the initial relaxation calculations started with the nucleobase molecules lying flat above the *h*-BN sheet with a vertical distance of 3.5 Å, which is characteristic for DNA-graphite hybrid. In the geometry optimization of the adsorption state, we used the procedure of Gowtham *et al.*,[25] where the rotational energy scan and the vertical energy scan were carried out in turn.

III. Results and discussion

The optimized configurations of five nucleobases adsorbed on the *h*-BN sheet are shown in Fig. 2. It can be seen that all five nucleobases exhibit the same *AB*-stacking-like arrangement on the *h*-BN sheet: the primary hexagonal ring of the bases prefers a nearly planar Top^N configuration on the *h*-BN sheet (with a tilt angle less than 3° with respect to the *h*-BN sheet, as induced by the attached methyl group), and the two N atoms of the primary hexagonal ring and the side O atom are right on top of the B atoms of the underlying BN hexagonal ring. The resulting stacking arrangement is similar to the *AB*-stacking-like adsorption configurations of adenine, thymine, and uracil on graphene (a homogeneous surface), but is quite different from those of guanine and cytosine on graphene.[25] Moreover, it is also distinctly different from the typical *AA′* stacking of *h*-BN phase (*i.e.*, all B atoms on top of N atoms and *vice versa*). Notably, the geometries of adsorbed nucleobase molecules remain essentially unchanged with respect to the corresponding gas-phase ones, which suggests a weak interaction (or physisorption) between adsorbates and the BN sheet, similar to the case of DNA nucleobases adsorption on graphite.

The difference in stacking sequences of nucleobases on *h*-BN sheet and graphene implies different interaction modes, which is sensitive to the nature of the template (*e.g.*, homogeneous or heterogeneous). For nucleobase molecules on the *h*-BN sheet, the preferred stacking arrangement (Fig. 2) leads to a maximum polar electrostatic interaction between nucleobases and sheet, and thus is mainly dependent on the polarity of the underlying *h*-BN sheet, but irrespective of the biological properties of nucleobases. It is expected that these nucleobases have well-defined and homogeneous adsorption patterns on the *h*-BN sheet, facilitating DNA self-assembly or pairing. This is a major advantage of *h*-BN sheet over graphene as a

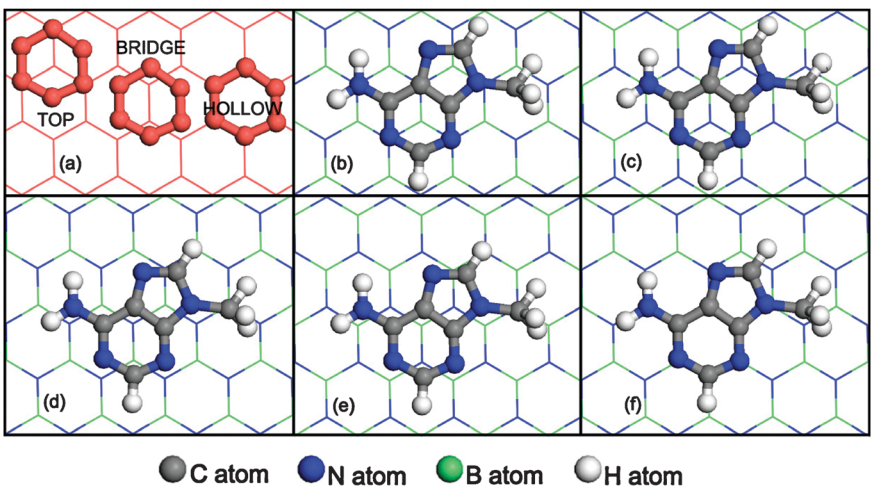

Fig. 1 (Color online) (a) The symmetry adsorption sites of a primary nucleobase hexagonal ring on the *h*-BN sheet: top, bridge and hollow. Initial top adsorption configurations (b) Top^B and (c) Top^N, where the center of the nucleobase hexagonal ring is on top of the B atom or N atom of the BN sheet. Initial bridge adsorption configurations (d) $bridge^{NB}$ and (e) $bridge^{BN}$, where the center of the nucleobase hexagonal ring is at the bridge site of the B–N bond. (f) Initial hollow adsorption where the center of the nucleobase hexagonal ring is on top of the center of the BN hexagonal ring.

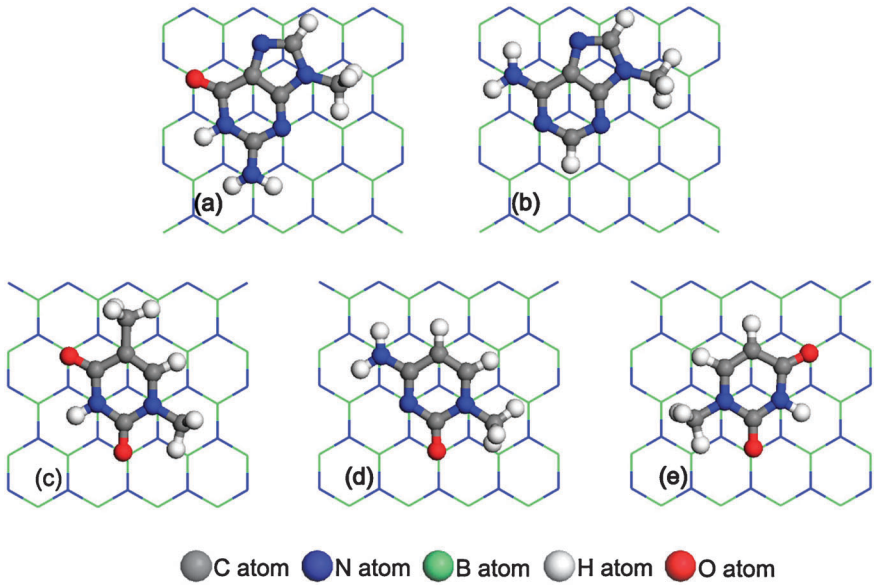

Fig. 2 (Color online) Optimized configurations of nucleobases adsorbed on *h*-BN sheet: (a) guanine, (b) adenine, (c) thymine, (d) cytosine, (e) uracil.

platform in the researches of biology, medicine and life science. On non-polar graphene, the π–π repulsion between graphene and adsorbates leads to the stacking arrangement more sensitive to the adsorbed nucleobases (*i.e.*, structures and properties).[25] The reason is that delocalized π states in graphene are not easily polarized.[28]

The *h*-BN sheet, as a polar material, has a nonuniform charge distribution and polarization anisotropy. This, to a large extent, determines the detailed orientation and behavior of adsorbates, especially macromolecules, on the substrate. A potential energy surface (PES) scan for all nucleobase adsorptions was further performed to explore the surface potential distribution and the binding mode, where the relaxed nucleobases were translated along the lattice vectors of the *h*-BN sheet in steps of 0.247 Å (*i.e.*, the entire unit cell is covered by a mesh of 10 × 10 scan points). As an example, the PES plot for adenine on the *h*-BN sheet is shown in Fig. 3. Compared with the case of adenine adsorbed on graphite,[28] the calculated PES on the *h*-BN sheet exhibits significant anisotropy resulting from the lower symmetry of the nucleobases and the polarization anisotropy of the *h*-BN sheet. The energy barrier is larger than the strength of intermolecular hydrogen bonds,[28] ranging from 0.17 to 0.30 eV. Even at room temperature, these energy barriers can considerably affect the diffusion of the adenine molecule on *h*-BN sheet, restricting its movement to certain directions (with lower diffusion barrier). This finding could be very important for understanding the self-assembly process of DNA/RNA on the BN template.

We further clarified the interaction between the nucleobase molecule and the BN sheet by calculating the adsorption energy and distance of the nucleobase molecule. Herein, the adsorption energy is defined as

$$E_{ads} = E_t(\mathrm{BN}) + E_t(\mathrm{molecule}) - E_t(\mathrm{molecule} + \mathrm{BN}),$$

where E_t(BN), E_t(molecule) and E_t(molecule + BN), respectively, denote the total energies of the *h*-BN sheet, isolated

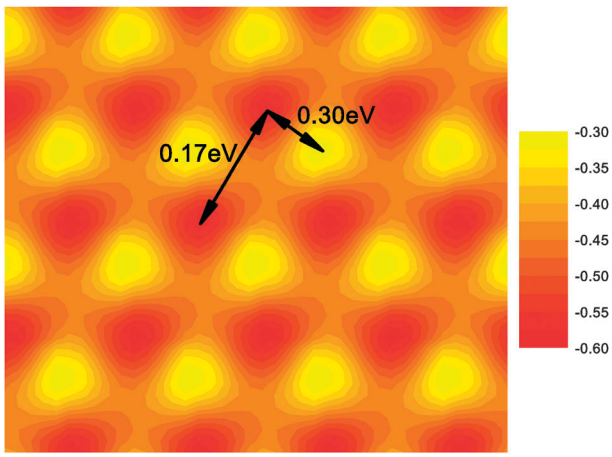

Fig. 3 (Color online) Potential energy surface (PES) (in eV) for adenine adsorbed on the *h*-BN sheet. Approximately, a 4 × 4 repetition of the unit cell is shown. The highest energy difference on the PES is about 0.30 eV, and the energy barrier between the two adjacent global minima is about 0.17 eV.

nucleobase molecule, and *h*-BN sheet with the nucleobase molecule.[29] The adsorption energies and equilibrium distances of the five nucleobases on the *h*-BN sheet were given in Table 1.

It can be seen that the adsorption energies of nucleobases on the *h*-BN sheet are in the range of 0.50 to 0.69 eV per molecule, which are much larger than those of gas molecules physisorbed on solid surface (0.01–0.1 eV per molecule), but less than those of the molecule chemisorbed on solid surfaces (1–10 eV per atom). Interestingly, the adsorption energies are close to those of glycine or adenine on Cu surface[30,31] and those of nucleobases on polarized silica derived surfaces.[32] However, the adsorption mechanism of different organic molecules on the same surface could be very different. For example, the binding of glycine to the Cu(110) surface mainly comes from the

Table 1 Adsorption energies (E_{ads}) and equilibrium distances (D_{eq}) between the molecule and the BN sheet for the five DNA/RNA nucleobases on the *h*-BN sheet

Nuclebase	E_{ads}/eV	D_{eq}/Å
guanine (G)	0.69	3.0
adenine (A)	0.58	3.1
thymine (T)	0.56	3.0
cytosine (C)	0.54	3.1
uracil (U)	0.50	3.1

hybridization of the N $2p_z$ orbital with the metal 3*d* band,[30] whereas the adsorption of adenine on Cu(110) surface can be attributed to the electrostatic interaction between substrate and adsorbate.[31] This clearly demonstrates that the interaction between biologically active molecules and solid surface is very complicated, even for similar adsorption processes or similar binding energies. Especially, we get the same sequence of the adsorption energies on polarized *h*-BN sheet (*i.e.*, G > A > T > C > U) as those for the five nucleobase molecules on graphene,[25] CNTs[33] or silica derived surfaces.[32] However, the identical nucleobase molecules have higher adsorption strength as compared to the case of their adsorption on graphene (about 0.44–0.61 eV per molecule[25]) and silica derived surface (about 0.37–0.47 eV per molecule[32]). On the other hand, the adsorption distances on *h*-BN sheet are shorter than those in the nucleobase-graphene system (about 3.5 Å[25]), and longer than those in the nucleobase–silica-derived system (about 2.9 Å[32]). These indicate that the interaction mechanism of nucleobase molecules with *h*-BN sheet is different from that of nucleobase molecules with graphene (*i.e.*, the π–π interaction[25,26]) or silica derived surface.[32]

More detailed information regarding interaction mechanism between nucleobases and *h*-BN sheet can be obtained from the analysis of electronic structure. In what follows we take adenine on *h*-BN sheet as an example. Fig. 4 shows the density of states (DOS) of the adenine-adsorbed BN sheet, pristine *h*-BN sheet and isolated adenine molecule. It can be seen that the DOS around the Fermi energy for the adsorption system may be approximately regarded as a simple sum of those of *h*-BN sheet and adenine. No new prominent hybridized peaks appear around the Fermi energy, which is different from the case of glycine on Cu(110) surface (*i.e.*, the orbital hybridization).[30] After adsorption, the effective band gap of the hybrid system is reduced to 3.585 eV. This is quite close to the gap between the highest occupied molecular orbital (HOMO) and lowest unoccupied molecular orbital (LUMO) of isolated adenine (3.643 eV). In Fig. 5, the isosurfaces of the partial charge density distribution are presented to more clearly characterize the HOMO and LUMO of the nucleobase, the top of the valence bands and the bottom of the conduction bands of the adenine-*h*-BN system. It can be seen that the nature of the HUMO and LUMO is basically unchanged upon the adsorption. Meanwhile, we do find a minor hybridization (Note that the isovalue of the partial charge density distribution is chosen as small as 0.002 e $Å^{-3}$.) Between these molecular orbitals with the p_z orbitals of *h*-BN. This, together with the fact that the geometry of adsorbed adenine remains almost unchanged in the adsorption process, confirms that the adsorption of adenine on *h*-BN sheet is not chemical in essence. In other words, the interaction between the adenine and *h*-BN sheet is too weak to change the characteristic electronic properties of adsorbate and adsorbent, just like the case of nucleobases on graphite, where the van der Waals contribution to the electronic structure could be negligible.[26] The above results indicate that the monolayer *h*-BN sheet may be used as the quasi-inert template for the self-assembly of DNA base molecules. This proposal was supported by a recent experiment, where high-concentration BN nanotubes (BNNTs) aqueous solutions were fabricated to study the pronounced interaction between DNA and BNNTs.[34]

The overall picture of the binding between adenine and BN sheet is further confirmed by analyzing the charge density difference upon adsorption. As shown in Fig. 6, there is no net charge transfer in a rather large range between adsorbate and adsorbent (*i.e.*, the adenine and *h*-BN sheet), compatible with the data of Mulliken charge analysis. This is distinctly different from the case of the adenine adsorption on Cu(110) surface, where the binding is mainly attributed to a

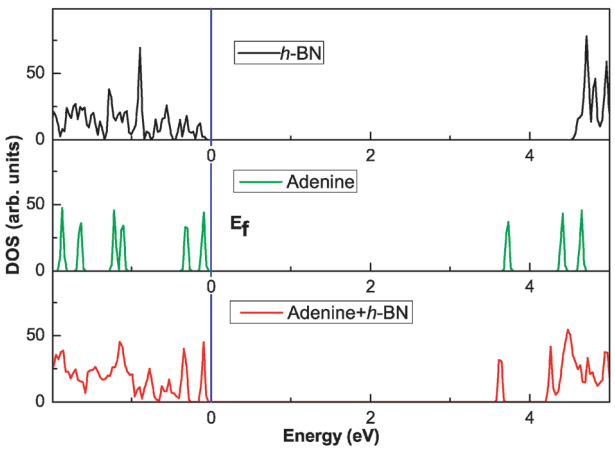

Fig. 4 (Color online) Density of states (DOS) for the adenine-adsorbed *h*-BN sheet (red solid line), isolated adenine molecule (green dashed line), and pristine *h*-BN sheet (black solid line). Energy zero is at the Fermi level (denoted as a blue solid vertical line).

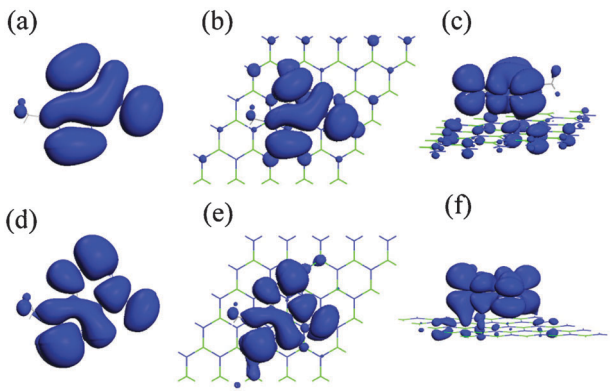

Fig. 5 (Color online) Isosurfaces of partial charge density distribution of selected orbitals: HUMOs of (a) isolated adenine and the top of the valence bands of adenine adsorbed *h*-BN ((b) top view and (c) side view), LUMOs of (d) isolated adenine and the bottom of the conduction bands of adenine adsorbed *h*-BN ((e) top view and (f) side view). The isodensity surfaces of 0.002 e $Å^{-3}$ are shown here.

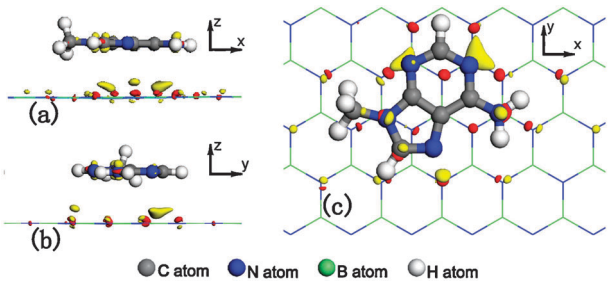

Fig. 6 (Color online) Charge density difference between the adenine-adsorbed *h*-BN sheet and the pristine *h*-BN sheet plus isolated adenine molecule. (a,b) side view; (c) top view. Isodensity surfaces for electron accumulation/depletion of ±0.005 e/Å^3 are displayed in red (+)/yellow (−).

charge-transfer-dependent electrostatic interaction.[31] It is found that for adsorption on the *h*-BN sheet, the charge redistribution only occurs in the intra-adenine molecule and the intra-sheet (as shown in Fig. 6). Thus the mutual polarization effects, compatible with the stacking arrangement of adenine on *h*-BN sheet mentioned above, become important and pronounced. As a consequence, an electrostatic interaction between adenine and *h*-BN sheet is induced by the charge redistribution, which determines the bonding.

In order to understand why different adsorption energies are found for the different base molecules, we analyze the charge density difference between the optimized hybrid systems and the pristine *h*-BN sheet plus isolated nucleobases as shown in Fig. 7. It can be seen that the polarization of the "pyrimidine ring" is stronger than that of the side groups or atoms during adsorption because the charge density changes of the former are more significant. An immediate and important consequence is that the five nucleobases containing identical "pyrimidine ring" have the same stacking arrangement (Fig. 7) and approximate adsorption energies (See Table 1) on the *h*-BN sheet, which may be a unique property of heterogeneous template application in the DNA self-assembly.

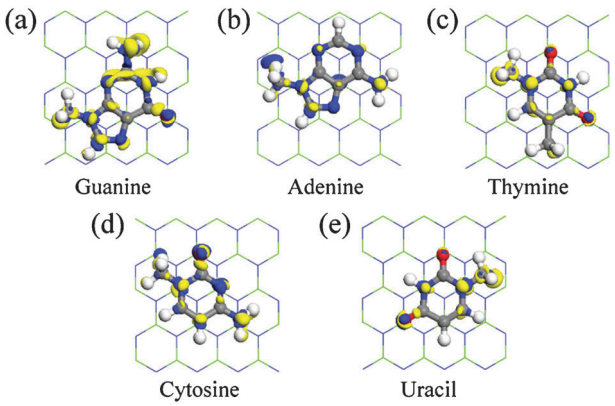

Fig. 7 (Color online) Charge density difference between the optimized hybrid systems and the pristine *h*-BN sheet plus isolated nucleobases. Isodensity surfaces for electron accumulation/depletion of ±0.003 e Å^{-3} are displayed in blue(+)/yellow(−). To clearly illustrate the contribution of intra-molecular charge redistribution to the adhesion, the charge density of the *h*-BN sheet is not given.

On the other hand, the interaction mechanism of mutual polarization in nature determines that the effects of side groups and atoms of nucleobases, which are slightly polarized, should not to be ignored. A typical example is that the adhesive forces of the five nucleobases on the *h*-BN sheet present a proper sequence: G > A > T > C > U (See Table 1). From Fig. 7, we can see that those atoms with higher electronegativity (*i.e.*, N and O with respect to C of hexagon or pentagon, C with respect to H of CH_2) induce more pronounced charge redistribution than the others. So it is reasonable to qualitatively deduce that: (1) purine bases generally have stronger adhesive force than pyrimidine bases because of one more pentagon formed by extra C and N atoms; (2) the extra O atom leads to a larger binding energy of guanine than adenine; (3) the effects of extra O and C atoms of thymine obviously exceed that of extra N atom of cytosine, and the contribution of N atom of cytosine is somewhat larger than that of O of uracil. The latter can be easily seen from the more significant charge redistribution of around N and O atoms in cytosine than that around O atoms in uracil. Consequently, we get the same sequence of adhesion of nucleobases on the *h*-BN sheet (G > A > T > C > U) from the mutual polarization analysis, as that of the adsorption energies (Table 1).

To complete our discussion, we also explore the perpendicular adsorption of nucleobases on the *h*-BN sheet, where nuclebases interact with the boron sites of *h*-BN *via* the lone pairs of basic sites (N, NH and CH). Herein, we take the adenine as an example. Fig. 8a–d show the optimized structures with the corresponding adsorption energies of 0.27 eV, 0.27 eV, 0.30 eV, and 0.21 eV. These energies are much smaller than that (0.58 eV) of the planar adsorption structure (shown in Fig. 2b). Similar to the adsorption of adenine on silica derived surfaces without the Na^+ cation,[32] the face-to-face orientation appears to be the preferred adsorption mode, since most atoms of the nuclebases are relatively close to the *h*-BN surface in this case. In addition, it is interesting to compare nucleobase adsorption on *h*-BN surface with that on boron nitride nanotubes (BNNTs).

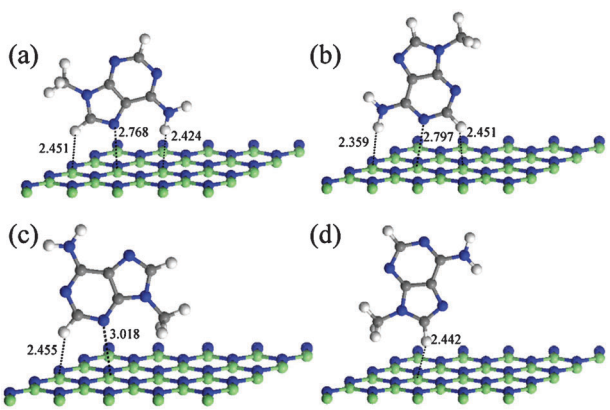

Fig. 8 (Color online) Optimized structures of adenine adsorbed on *h*-BN sheet in the perpendicular mode. Gray, blue, cyan, and white spheres represent C, N, B, and H atoms, respectively. The listed numbers indicate the distance of some selected nearest neighbor atoms (in units of Å).

Recently, Mukhopadhyay *et al.* have studied the physisorption of nucleobases on (5,0) BNNT.[35] To understand the curvature effect, we further examine the adsorption of adenine on (8,0) and (12,0) BNNTs. The optimized structures are the same as that on the *h*-BN sheet, *i.e.* Top^N configuration. The adsorption energies are 0.32 eV (taken from ref. 35), 0.46 eV, and 0.54 eV for the adsorption on (5,0), (8,0) and (12,0) BNNTs respectively. It can be seen that the adsorption energy of the adenine molecule is substantially reduced with decreasing tube size, which can be understood from the planar structure of the molecule and its interaction mechanism with the BN structures analyzed above. Note that similar behavior has been previously observed for the adenine adsorption on CNTs and graphene.[36]

IV. Conclusion

Our *ab initio* calculations showed that all five nucleobases of DNA and RNA [*i.e.*, A, G (purine bases), and C, T and U (pyrimidine bases)] exhibit the same stacking arrangement on the *h*-BN sheet, irrespective of their biological properties. The N and O atoms of the nucleobases prefer to stay on top of B atoms of *h*-BN sheet, with a vertical distance of $\sim$3.1 Å. The adsorption energies, ranging from 0.69 to 0.50 eV, is in the order G > A > T > C > U, which is the same as the case of nucleobases on graphene and silica derived surfaces. The weak interaction of nucleobases with *h*-BN sheet is mainly attributed to the electrostatic interaction induced by mutual polarizations (*i.e.*, intra-molecule and intra-sheet charge re-distribution) of adsorbates and adsorbent, which is somewhat stronger than the π–π interaction between the nucleobases and graphene. Such interaction between nucleobases and *h*-BN sheet, on the one hand, does not change the fundamental natures of DNA/RNA nucleobases and *h*-BN sheet, indicating that the *h*-BN sheet is a promising template for DNA/RNA-related research, such as self-assembly. On the other hand, it immobilizes nuclebases on the sheet, facilitating the growth of a perfect DNA-BN hybrid for potential device applications in different environments.

Acknowledgements

This work was supported by the Ministry of Science and Technology of China (Grant Nos. 2011CB606405, 2011CB921901 and 2009CB929400), the National Natural Science Foundation of China (Grant No. 11074139).

References

1 J. P. Ferris and G. Ertem, *Science*, 1992, **257**, 1387.
2 G. Ertem and J. P. Ferris, *Nature*, 1996, **379**, 238.
3 G. Ertem and J. P. Ferris, *J. Am. Chem. Soc.*, 1997, **119**, 7197.
4 G. Ertem and J. P. Ferris, *Origins Life Evol. Biospheres*, 2000, **30**, 411.
5 N. J. Tao, J. A. DeRose and S. M. Lindsay, *J. Phys. Chem.*, 1993, **97**, 910.
6 Q. Chen, D. J. Frankel and N. V. Richardson, *Langmuir*, 2002, **18**, 3219.
7 T. Uchihashi, T. Okada, Y. Sugawara, K. Yokoyama and S. Morita, *Phys. Rev. B: Condens. Matter*, 1999, **60**, 8309.
8 J. Adamcik, S. Tobenas, G. Di Santo, D. Klinov and G. Dietler, *Langmuir*, 2009, **25**, 3159.
9 C. R. Clemmer and T. P. Beebe, *Science*, 1991, **251**, 640.
10 K. Watanabe, T. Taniguchi and H. Kanda, *Nat. Mater.*, 2004, **3**, 404.
11 D. Pacilé, J. C. Meyer, Ç. Ö. Girit and A. Zettl, *Appl. Phys. Lett.*, 2008, **92**, 133107.
12 W.-Q. Han, L. J. Wu, Y. M. Zhu, K. Watanabe and T. Taniguchi, *Appl. Phys. Lett.*, 2008, **93**, 223103.
13 M. Terrones, J. M. Romo-Herrera, E. Cruz-Silva, F. Lopez-Urias, E. Munoz-Sandoval, J. J. Velazquez, H. Terrones, Y. Bando and D. Golberg, *Mater. Today*, 2007, **10**, 30.
14 C. Jin, F. Lin, K. Suenaga and S. Iijima, *Phys. Rev. Lett.*, 2009, **102**, 195505.
15 J. C. Meyer, A. Chuvilin, G. Algara-Siller, J. Biskupek and U. Kaiser, *Nano Lett.*, 2009, **9**, 2683.
16 J. Li, G. Zhou, Y. Chen, B.-L. Gu and W. H. Duan, *J. Am. Chem. Soc.*, 2009, **131**, 1796.
17 F. W. Zheng, G. Zhou, Z. R. Liu, J. Wu, W. H. Duan, B.-L. Gu and S. B. Zhang, *Phys. Rev. B: Condens. Matter Mater. Phys.*, 2008, **78**, 205415.
18 A. Du, Y. Chen, Z. Zhu, G. Lu and S. C. Smith, *J. Am. Chem. Soc.*, 2009, **131**, 1682.
19 X. W. Tang, S. Bansaruntip, N. Nakayama, E. Yenilmez, Y. L. Chang and Q. Wang, *Nano Lett.*, 2006, **6**, 1632.
20 N. Mohanty and V. Berry, *Nano Lett.*, 2008, **8**, 4469.
21 G. Kresse and J. Furthmüller, *Comput. Mater. Sci.*, 1996, **6**, 15.
22 G. Kresse and J. Furthmüller, *Phys. Rev. B: Condens. Matter*, 1996, **54**, 011169.
23 D. Vanderbilt, *Phys. Rev. B: Condens. Matter*, 1990, **41**, 7892.
24 J. P. Perdew and A. Zunger, *Phys. Rev. B*, 1981, **23**, 5048.
25 S. Gowtham, R. H. Scheicher, R. Ahuja, R. Pandey and S. P. Karna, *Phys. Rev. B: Condens. Matter Mater. Phys.*, 2007, **76**, 033401.
26 Y. V. Shtogun, L. M. Woods and G. I. Dovbeshko, *J. Phys. Chem. C*, 2007, **111**, 18174.
27 To show that the 5 ×5 × 1 supercell is big enough to exclude the influence of the lateral interaction of nucleobases on the adsorption energies, we have performed the calculation for adenine adsorption on *h*-BN sheet in the 6 × 6 × 1 supercell. The calculated adsorption energy is 0.57eV, which is only 0.01eV smaller than that in the 5 × 5 × 1 supercell case for the adenine molecule.
28 F. Ortmann, W. G. Schmidt and F. Bechstedt, *Phys. Rev. Lett.*, 2005, **95**, 186101.
29 We check the validity of our definition of the adsorption energy by using the asymptotic approach[25] to calculate the adsorption energies. Again, we take the adenine adsorption as an example. Our calculation using the asymptotic approach yields an adsorption energy of 0.582 eV, which is almost the same as the calculated value following the definition in our work. This shows that in the present case, our definition of the adsorption energy can give reasonably accurate results.
30 M. Nyberg, J. Hasselström, O. Karis, N. Wassdahl, M. Weinelt, A. Nilsson and L. G. M. Pettersson, *J. Chem. Phys.*, 2000, **112**, 5420.
31 M. Preuss, W. G. Schmidt and F. Bechstedt, *Phys. Rev. Lett.*, 2005, **94**, 236102.
32 P. Mignon, P. Ugliengo and M. Sodupe, *J. Phys. Chem. C*, 2009, **113**, 13741.
33 A. Das, A. K. Sood, P. K. Maiti, M. Das, R. Varadarajan and C. N. R. Rao, *Chem. Phys. Lett.*, 2008, **453**, 266.
34 C. Y. Zhi, Y. Bando, W. Wang, C. C. Tang, H. Kuwahara and D. Golberg, *Chem.–Asian J.*, 2007, **2**, 1581.
35 S. Mukhopadhyay, S. Gowtham, R. H. Scheicher, R. Pandey and S. P. Karna, *Nanotechnology*, 2010, **21**, 165703.
36 S. Gowtham, R. H. Scheicher, R. Pandey, S. P. Karna and R. Ahuja, *Nanotechnology*, 2008, **19**, 125701.

